Coastal Dynamics 2017
Paper No. 69

Rip currents vorticity scaling

Eric Barthélemy[1]

Abstract

Rip currents as originally studied by Bowen (1969) can be viewed as part of vortical dipoles structures. A wave averaged vorticity equation is derived from the wave average shallow water equations. The former has both a vorticity source term due to breaking and a dissipation term by bottom friction. By modeling the source term with spatially variable breaker index γ we derive a new semi-empirical model which is validated by basin experiments of rip currents. A scaling of rip current velocity is given showing the importance of the alongshore non-uniformity, the wave period and the slope of the beach. We also show that the constant γ option leads to much stronger rip currents.

Key words: rip current, vorticity, analytical modeling, breaking wave dissipation, breaker index, scaling

1. Introduction

Rip currents occur in many different settings (MacMahan et al., 2006; Dalrymple et al., 2011) in the form of more or less narrow seaward jets that are part of vortical near-shore circulations. They are most of the time associated with underlying bathymetric features called rip channels which show quasi-rhythmic spacing along the coastline. While longshore currents can only occur under the forcing of oblique breaking waves, rip currents can be generated by quasi frontal waves (shore normal wave rays). Transfer of breaking wave momentum to surf zone mean circulations can result in large scale macro-vortices such as rip currents (Long & Ozkan-Haller, 2005; Dalrymple et al., 2011).

Peregrine (1998) showed that at the wave scale, differential wave breaking due to wave height gradients along the crest of the wave breaker can be a source of instantaneous vorticity, each edge of the finite breaking bore crest shedding vortices (Peregrine, 1999; Bonneton et al., 2010; Clark et al., 2012). This small scale vorticity rearranges into large scale vorticity. Rip cells are of that nature and were comprehensively modeled by Bowen (1969).

Numerical modeling strategies for rip currents are either based on intra-phase wave models or on depth averaged equations based on the radiation stress formalism (Longuet-Higgins & Stewart, 1964). In the first category, wave breaking is parametrized (Madsen et al., 1997I; Kennedy et al., 2000; Cienfuegos et al., 2006) or intrinsically computed in the form of shocks when the nonlinear shallow water equations are used (Suarez et al., 2013). The first category usually requires to set up a wave driver to compute wave evolution and close the radiation stresses evaluations (Long & Ozkan-Haller, 2005; Bruneau et al., 2011). In wave drivers, bathymetric induced wave breaking parametrization can based on a constant breaker index $\gamma = H/h$ where H and h are respectively the local wave height and water depth. Another shortcoming in time and depth average modeling will often be the closure assumption for the radiation stress estimators. Indeed most of the time they are closed using linear wave theory even in the surf zone and known to overestimate, for instance in 1D simulations undertow currents (Michallet et al., 2011), although radiation stress estimators for nonlinear waves are available (Madsen et al., 1997II; Michallet et al., 2011).

In the present study we assess how modeling options such as spatially constant γ and linear wave radiation stresses estimates affect velocity magnitude of a steady rip current cell. We also investigate how

1 LEGI, University of Grenoble Alpes, France. Eric.Barthelemy@grenoble-inp.fr

the wave period, the alongshore depth non-uniformity, control the rip cell vorticity level. To unravel these issues a model which is an extension of that of Bowen (1969) is well suited since it encompasses the main physics of rip cells.

2. A semi-analytical model

Even though some studies (Marchesiello et al., 2015) indicate that rip currents should be modeled with 3D equations most of the physics is mainly 2D. Rip currents are circulation cells roughly 1.5 the width of the surf zone in size, which is clearly a shallow water flow. Moreover measured in-situ vertical profiles of rip currents (MacMahan et al., 2006) indicate a quasi vertical uniform time average current except for the surface Stokes drift. Therefore the subsequent analysis will be based on the Barré de Saint Venant equations.

After splitting the unknown functions in wave averaged components and fluctuating orbital components, the Barré de Saint Venant equations are wave averaged to yield (Bonneton at al., 2010):

$$\partial_t \boldsymbol{u} + \boldsymbol{u}\nabla(\boldsymbol{u}) + g\,\nabla\eta = D\,\boldsymbol{e}_k - \nabla\tilde{J} - \overline{\tilde{\omega}\,\tilde{\boldsymbol{u}}} \times \boldsymbol{e}_z - \frac{C_f}{h}\,\boldsymbol{u}\,|\boldsymbol{u}|$$

$$\partial_t h + \nabla(\boldsymbol{u}\,h) = -\nabla\tilde{\boldsymbol{M}}$$

where all functions are wave-averaged quantities that vary on time scales much larger than the wave period and where,

- $\boldsymbol{u} = [u\ v]$ is the time averaged horizontal velocity field and $\tilde{\boldsymbol{u}}$ the orbital motion or wave field;
- $n(x.u.t)$ is the mean free position and $h(x.u.t) = h_0(x.u) + n(x.u.t)$ is the mean water depth
- with h_0 the water depth at rest;
- $\nabla = [\partial_x\ \ \partial_y]$ is the gradient operator in the $(x.u)$ horizontal plane;
- the over-line is the wave averaging operator and the tilde refers to the fluctuating orbital component;
- $\tilde{\boldsymbol{M}}$ is the wave induced mass flux (Stokes drift): $\tilde{\boldsymbol{M}} = [\overline{\tilde{u}\tilde{n}}\ \overline{\tilde{v}\tilde{n}}]$
- $D(x.u.t)$ is the so-called dissipative force (Bonneton et al., 2010; Weir et al. (2011);
- $\boldsymbol{e}_k$ is the unit vector tangent to wave rays and $\boldsymbol{e}_z$ is the vertical unit vector pointing in the opposite direction to $\boldsymbol{g}$, the gravity acceleration;
- $\tilde{\omega}$ is orbital motion contribution to the vorticity or wave-scale vorticity;
- $\overline{\tilde{\omega}\,\tilde{\boldsymbol{u}}}$ is the wave scale vorticity diffusion by the wave field $\tilde{\boldsymbol{u}}$;
- C_f is the friction factor in the quadratic friction law
- $\tilde{J}$ the wave kinetic energy

An wave averaged vorticity equation is derived by taking the curl of (1),

$$\partial_t \omega + \nabla(\omega\,\boldsymbol{u}) = \nabla \times (D\,\boldsymbol{e}_k)\cdot\,\boldsymbol{e}_z - \nabla(\overline{\tilde{\omega}\,\tilde{\boldsymbol{u}}}) - \beta\,\nabla \times \left(\frac{\boldsymbol{u}}{h}\right)\cdot\boldsymbol{e}_z$$

where, ω is the wave averaged vorticity (vertical component), we assume β is constant. This friction parameter is defined by $\beta = C_f U_{rms}$ where U_{rms} is the root mean square of the orbital velocity magnitude. The left hand-side of (2) is the vorticity change in time and advection by the mean currents. On the right-hand side, the first term is a source term of average vorticity generation by wave breaking, the second term is the mixing/diffusion of wave vorticity by orbital wave motion and the third is a sink term of average vorticity dissipation by bottom friction. These equations are very similar to those of Weir at al. (2011).

In the case of frontal waves with negligible refraction the wave rays are orthogonal to the bathymetric lines which implies,

$$\nabla \times (D\,\boldsymbol{e}_k)\cdot\boldsymbol{e}_z \simeq \partial_y D \tag{3}$$

Measurements and numerical simulations tend to show that $\nabla(\overline{\tilde{\omega}\,\tilde{\boldsymbol{u}}})$ in (2) and $\nabla\tilde{\boldsymbol{M}}$ in (1) are negligible. We also assume a steady forcing and therefore steady wave averaged quantities. In this case it is reasonable to think that the amount of vorticity generated by wave breaking is balanced by the amount of vorticity

destroyed by friction. Under such assumptions the mass conservation of (2) reduces to,

$$\nabla(\boldsymbol{u}\, h) = 0 \tag{4}$$

which ensures the existence of a transport stream function ψ such that the system (2) reduces to,

$$\begin{gathered} \boldsymbol{u}\, h = \nabla\psi \times \boldsymbol{e}_z \\ \nabla.\left(\frac{1}{h^2}\,\nabla\psi\right) = -\frac{1}{\beta}\, S(x,y) \\ S(x,y) = \partial_y D \end{gathered} \tag{5}$$

This is closely linked to Bowen's expressions (Bowen, 1969). Bowen assumed γ to be constant (no h and T dependency) and the dissipative force was computed from the curl of the radiation stress evaluated as if the breakers were linear waves. This led (Bowen, 1969) to write,

$$S_B = \left(\frac{g\,\gamma^2}{4}\right)\,\partial_{xy} h \tag{7}$$

where it is also assumed that the beach is close to a planar beach of slope $\partial_{\perp} h \simeq m$.

The difference in our approach is in how the dissipative term is modeled. We compute the dissipative force as if the breakers were bores, a consistent approach with the existence of weak shock solutions in the shallow water equations. This gives,

$$D = \frac{\Delta_b/\rho}{C\, h} \simeq \frac{g}{4\, C\, T}\,\frac{H^3}{h^2} \simeq \frac{g^{1/2}}{4\, T}\,\gamma^3\, h^{1/2}$$

where Δ_b is the wave average bore induced wave energy dissipation (hydraulic jump dissipation), $C \simeq \sqrt{g\, h}$ the shallow water wave speed, T the peak wave period and ρ the fluid specific gravity. This expression of the dissipative force calls for a model for γ.

We use the empirical formulation of Raubenheimer et al. (1996),

$$\begin{gathered} \gamma = a + b\, I_b\, \left(\frac{h}{h_b}\right)^{-1/2} \\ I_b = m\frac{L_b}{h_b} = \frac{m\, T\, g^{1/2}}{h_b^{1/2}} \end{gathered} \tag{9}$$

where h_b is the water depth at breaking point, I_b a kind of surf similarity parameter Svendsen (1987), L_b the wave length at the breaking point and a and b are dimensionless positive parameters. This choice implies that the forcing function S in (6) writes,

$$\begin{gathered} S(x,y) = K\, F\,(h/h_b)\;\partial_y h \\ K = \frac{g^{1/2}}{8 T h_b^{1/2}} \\ F\,(h/h_b) = \gamma^2\,\left(\frac{h}{h_b}\right)^{-1}\,\left[a\left(\frac{h}{h_b}\right)^{1/2} - 2\, b\, I_b\right] \end{gathered} \tag{10}$$

A useful approximation of the modulating function F, valid for 90% of the surf zone (see next section) writes,

$$F\,(h/h_b) \simeq -2\, b^3\, I_b^3\,\left(\frac{h}{h_b}\right)^{-2} \tag{11}$$

The Poisson-Helmholtz problem (6) with (10) is now entirely defined. Contrary to Bowen's study, where the left-hand side of (6) is spatially constant, in the present derivation the forcing function is not. We therefore resort to numerical methods to solve this boundary condition problem.

The problem (6) is solved with a standard 2D finite element software with Dirichlet boundary conditions:

$$\psi = 0 \tag{12}$$

on the boundaries of the rectangular domain. The input data is the bathymetry $h(x, y)$, but also the K constant (10).

3. **Results and discussion**

The semi-analytical model and its assumptions are tested on the tank experiments of Michallet et al. (2013) to which the reader is referred for extensive details. The experiments have been conducted in the LHF/ARTELIA 30x30 m wave basin. The ``offshore" end wall is made up of 60 independently controlled piston type wave-makers. The still water level at the wave-makers was $h_0 = 0.765$ m. Out of all the runs the specific random wave B2 run is used here: a significant wave height of $H_s = 0.18$ m and a peak period of $T_p = 3.5$ s.

The associated bathymetry is shown in figure 1 and 2. It is an overall cylindrical beach with mild alongshore gradients. It is a terrace type beach with the breaking point at the slope change (fig. 2). The slope of shoaling zone is roughly 1/20 and that of the surf-zone of 1/35. Waves were frontal incoming from the right with crests aligned with the alongshore direction. The average velocity field was measured by video recording drifter motions as explained in Castelle et al. (2010).

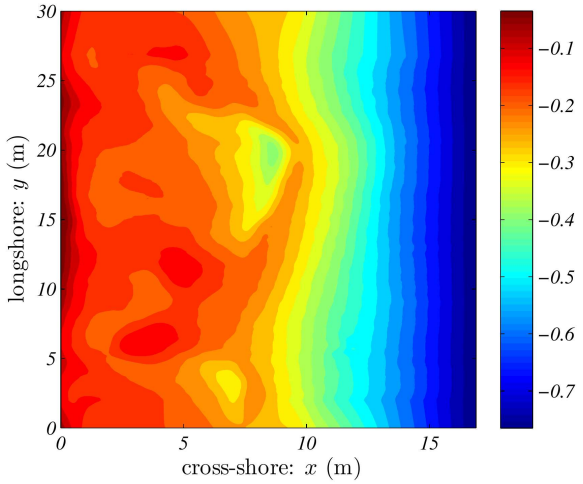

Figure 1. Bathymetric map with colormap in meters. $z = 0$ is the free surface plane at rest. Wave-makers are located on the right boundary at $x = 22$ m, shoreline at $x = 0$ m, breaking depth $h_b \simeq 0.3$ m, average shoaling slope $m = 1/20$.

Before we proceed to the circulation computations, we validate the formula (9) against the data of the laboratory measurements of Michallet et al. (2013). The data was collected on different cross-shore transects of the the laboratory beach and therefore with different cross-shore profiles (figure 2). Despite the scatter, the agreement in figure 3 is reasonable in the sense that the general trend is much better than that given by the Thornton & Guza (1983 formulation for instance. In the same figure 3 the approximation (11) of the modulating function F is shown to match fairly well on a large range of h/h_b.

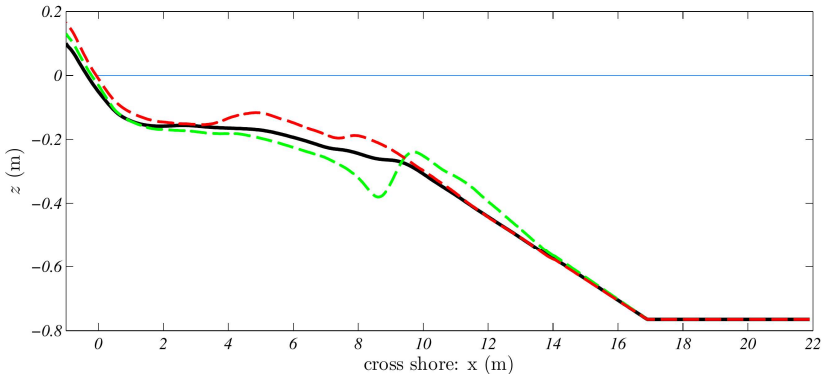

Figure 2. Cross-shore profiles at $y \simeq 20$ m (dashed green), $y \simeq 12$ m (dashed red) and longshore average (---). Wave-makers are located on the right boundary at $x = 22$ m, shoreline at $x = 0$ m, breaking depth $h_b \simeq 0.3$ m, average shoaling slope $m = 1/20$

The second stage is the validation of the semi-analytical model (6) with the experimental data. For that purpose the K of (10) was defined with the peak period, the depth h_b at the location where maximum H_s occurs along the transect. The slope m in I_b was defined by averaging the slope of the shoaling zone on various cross-shore transects. The comparison between the measurements and the semi-analytical model is plotted in figure 4.

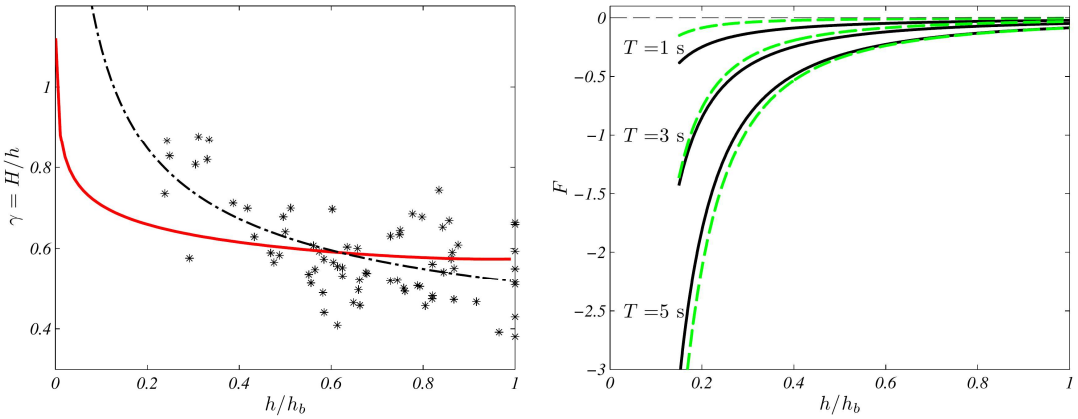

Figure 3. Left panel: breaking index γ with H the root mean square wave height. Laboratory data of Michallet et al. (2013): (∗) experimental data ($T_p = 3.5$ s) , (-.-.-): estimation with (9) with $a = 0.25$, $b = 0.2$ and $I_b = 1.34$; red (--) Thornton & Guza (83) with $B = 0.7$, $\gamma_b = 0.6$ and $m = 1/40$. Right panel: the forcing function F. Plain lines: formula (10) and dashed approximation: formula (11).

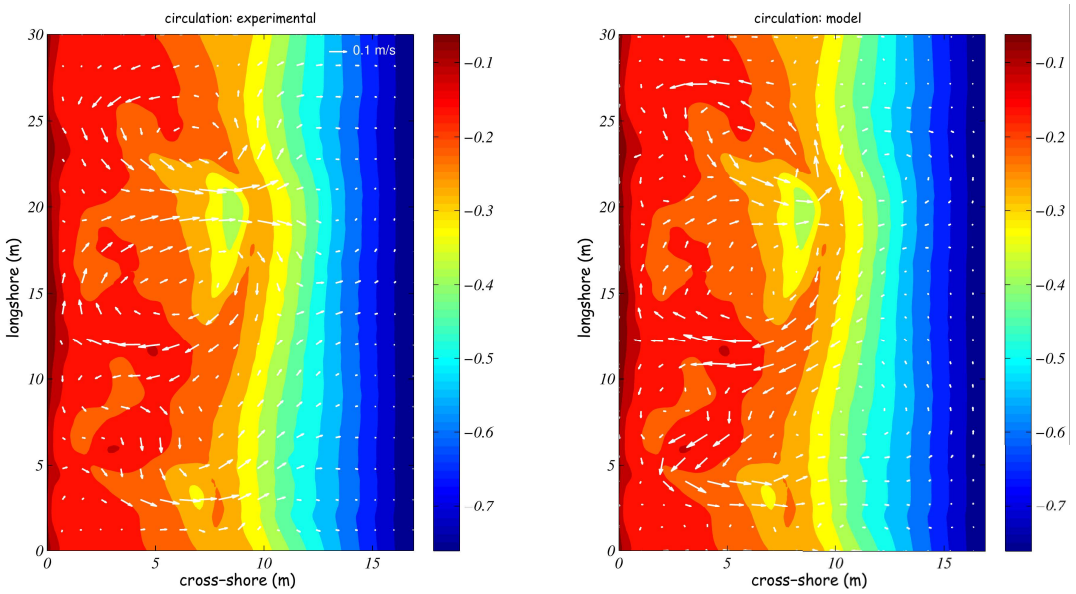

Figure 4. Experimental mean circulation and the semi-analytical model results. Semi-analytical model (6) and forcing function (10) with (9).The bathymetric color scale is in meters, $z = 0$ is the free surface at rest. $\beta = 0.05, h_b = 0.30$ $m = 1/20$.

The computed mean circulation pattern strongly resembles the experimental one and in addition the rip current magnitudes are close. Rip currents are located at $y \simeq 3$ m and $y \simeq 20$ m in both the experiments and the model. The gyre which center is located at ($x \simeq 7$ m, $y \simeq 23$ m) is slightly tilted in the simulation. The inshore feeder current at $u \simeq 12$ m is slightly stronger in magnitude in the model.

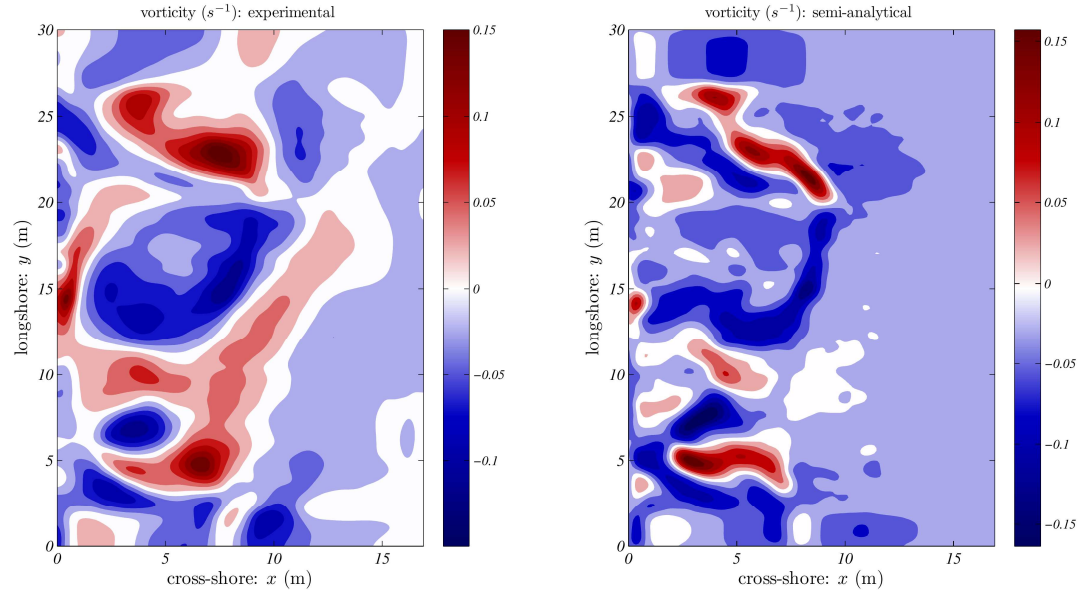

Figure 5. Experimental vorticity and predicted by the semi-analytical model. Model computed with equation (6) and forcing function (10) with (9}). $\beta = 0.05, h_b = 0.30, m = 1/20$.

The associated vorticity distribution is plotted in figure 5. Even though our semi-analytical model

is highly simplified, the ridges of maximum and minimum predicted vorticity are similar to the experimental ones both in magnitude and shape. The main differences lie in the broader size, due to diffusion, of the experimental vorticity patches. Diffusion in the the vorticity equation (2) could have been modeled by the term $\nabla(\widetilde{\omega}\,\widetilde{\boldsymbol{u}})$ not included here. This term models the horizontal mixing of the wave scale vertical vorticity by the wave orbital motion. Since our aim is more to understand the scalings for the vorticity and velocity, this test shows that our simple analytical model is able to capture the main features of the velocity and vorticity fields.

This model is now applied on the idealized non-dimensional case of Bowen (1969). The bathymetry is made of an overall plane beach with an off-shore rip-channel as shown on figure 6. The bathymetry $h(x,y)$ is therefore a plane beach with a mild alongshore gradient given by the expression,

$$\begin{aligned} h(x,y) &= h_0(x)\,\left(1-\epsilon\,\cos 2\pi y+\epsilon^2\,\cos 4\pi y\right) \\ h_0(x) &= m\,x \end{aligned} \tag{13}$$

where ϵ governs the magnitude of the alongshore gradient $\partial_y h$. The second sinusoidal term inside the brackets of (13) serves to narrow the rip channel. The alongshore non-uniformity ϵ is related to the alongshore depth standard deviation σ_z introduced by Feddersen & Guza (2003) and used by Castelle et al. (2010) by,

$$\epsilon \simeq \frac{\sigma_z}{h} \tag{14}$$

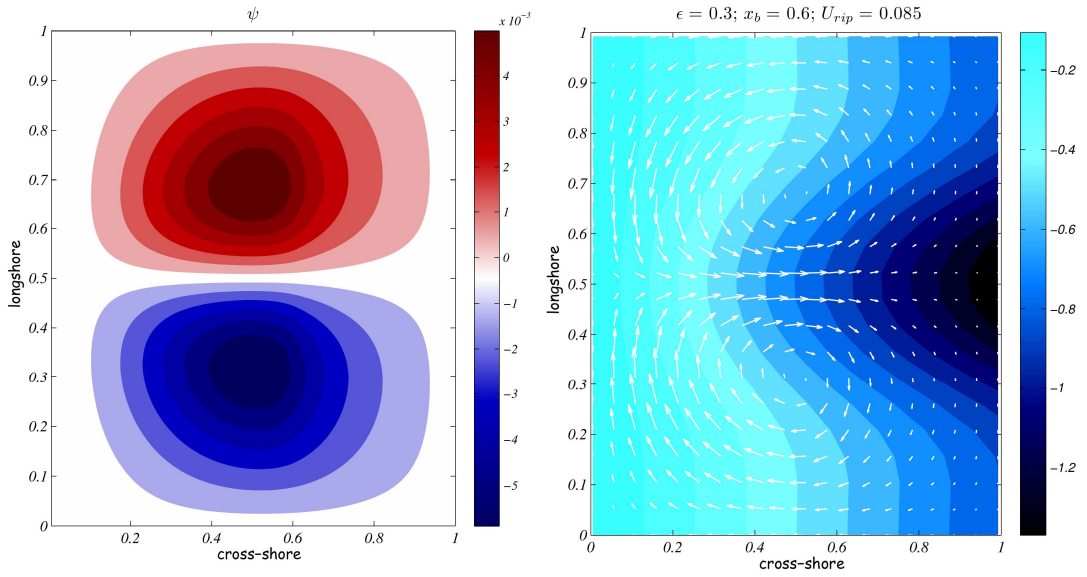

Figure 6. Model on Bowen's idealized bathymetry. Left panel: transport function ψ field. Right panel: the bathymetry overlaid with the velocity field. $x_b = 0.6$.

The figure 6 shows both the transport function ψ field and the resulting velocity field. As expected a narrow rip at $y = 0.5$ is formed due to a vorticity dipole forced by the bathymetric gradients in the middle of the rip channel. The neck of the rip current is very close to the breaker line at $x_b = 0.6$ and it is found to be the case for any x_b. On these grounds it is straightforward to show that the rip velocity magnitude scales as,

$$U_{rip} \propto \frac{b^3\,g^2}{4}\,\frac{\epsilon\,m^3\,T^2}{\beta} \tag{15}$$

in which the order of magnitude of $\partial_n h$ was chosen to be $\epsilon\, h/L$.

On the other hand the scaling from Bowen (1969) is,

$$U_B \propto \frac{g\,\gamma^2}{4}\,\frac{\epsilon\, m^2\, x_b}{\beta} \tag{16}$$

The rip current U_{rip} linearly increases with alongshore non-uniformity ϵ as exactly given by U_B of (16) and also shown experimentally by Castelle et al. (2010). In figure 7 the maximum rip velocities are plotted for both a Bowen type model and the present semi-analytical model. The linear trend was of course expected for both (15) and (16), but it is also noticeable that the Bowen model values are much larger than those of the present model. Our understanding is that it is a consequence of the constant breaker index γ and the linear wave radiation stress estimator for the breaking waves.

What differs between the (16) scaling of Bowen (1969) and the present (15) scaling is the relationship to the slope *m* of the beach. The slope dependency of U_{rip} in the present study is strong with a power 3 of *m* while for (16) it is quadratic. This is due to the fact that γ increases with *m* in (9) while Bowen choose a constant γ in the source term (7).

Moreover, the (15) scaling shows that as the wave period *T* increases the rip current also increases a behavior not given by (16). Indeed as the offshore steepness H_0/L_0 decreases due to the wave period increase, the surf similarity parameter I_b increases Svendsen (1987) in the forcing function (10) generating a stronger rip current.

More surprisingly the current U_{rip} order of magnitude of (15) is apparently independent of h_b and x_b, respectively the breaking point depth and cross-shore location. This is confirmed by the computation on the idealized case which shows little dependence on the non-dimensionnal rip velocity to the x_b position. On the contrary scaling (16) suggest the rip current velocity is x_b dependent.

The Froude number F_{rip} of the rip current close to the neck can easily be expressed,

$$F_{rip} = \frac{U_{rip}}{\sqrt{g\,h_b}} \sim \frac{b^3}{4}\,\frac{\epsilon\, m}{\beta}\, c_b\, I_b^2 \tag{17}$$

where $c_b\, is$ the shallow water wave speed at the breaking point.

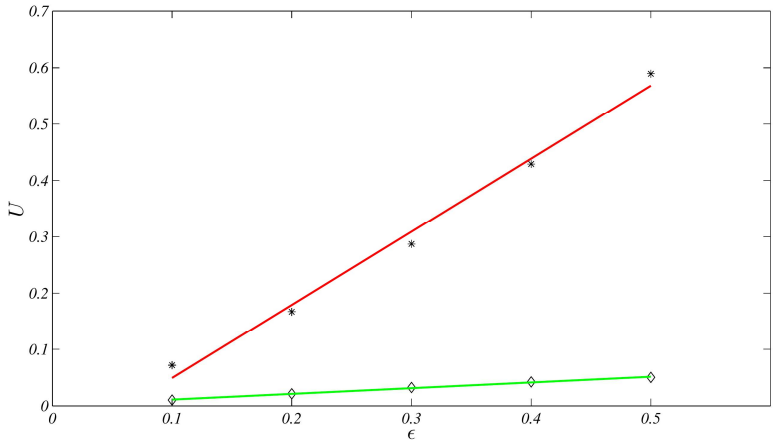

Figure 7. Rip velocity as a function of the alongshore non-uniformity. Bowen (1969) model with constant γ: ($\star$), linear fit in red; semi-analytical model with spatially variable γ: ($\diamond$), linear fit in green.

4. Conclusion

A semi-analytical model of rip current cells was derived on the assumption of an equilibrium between vorticity production by the differential breaking of waves controlled by the bathymetry and the destruction of vorticity by the bottom friction.

The wave driver in this semi-analytical model comes down to the prescription of a variable breaker index γ function. It is noticeable that the mean circulation that would be triggered by inhomogeneous wave amplitudes would lead to the same semi-analytical model.

The model was validated with tank experiments of Michallet et al. (2013) with a good match on the velocity field pattern and magnitude.

A scaling for the velocity at the neck of the rip naturally arise from the model and is compared with that of Bowen (1969). The scaling shows,

- a linear relationship with the alongshore non-uniformity in both models;
- a linear trend with the wave peak period in the semi-analytical model while no period dependency for Bowen (1969);
- that in both models rip velocity increases with the beach slope although not with the same power law.

While in the present study the non-dimensional case concerned an off-shore type of rip channel, future work will look into the characteristics of rip cells controlled by beach bathymetries with shoreline cusps.

Acknowledgements

This work is partly funded by the MEPIERA project of Grenoble INP and the VIGIECOT PEPS-AGIR of the University of Grenoble Alpes. We are indebted to H. Michallet who lead the LHF/ARTELIA basin experiments, for the fruitful discussions and for his craftmanship in plot fabrication! Our acknowledgments also go to Leandro Suarez Atias who contributed to make this work possible by the many discussions we had in the course of his PhD and to Ph. Bonneton for introducing us to the subject.

References

Bonneton P., N. Bruneau, B. Castelle, and F. Marche, 2010. Large-scale vorticity generation due to dissipating waves in the surf zone. *Discrete Contin. Dyn. Syst.*, Ser. B, 13(4):729–738.

Bowen A.J., 1969. Rip currents: 1. theoretical investigations. *Journal of Geophysical Research*, 74(23):5467–5478.

Bruneau N., P. Bonneton, B. Castelle, and R. Pedreros, 2011. Modeling rip current circulations and vorticity in a high-energy mesotidal-macrotidal environment. Journal of Geophysical Research: Oceans (1978–2012), 116(C7).

Castelle B., H. Michallet, V. Marieu, F. Leckler, B Dubardier, A. Lambert, C. Berni, P. Bonneton, E. Barthelemy, and F. Bouchette, 2010. Laboratory experiment on rip current circulations over a moveable bed: Drifter measurements. *Journal of Geophysical Research: Oceans*, 115(C12).

Cienfuegos R., E. Barthélemy, and P. Bonneton, 2006. A fourth order compact finite volume scheme for fully nonlinear and weakly dispersive Boussinesq-type equations. Part I : model development and analysis. *Int. J. Num. Meth. Fluids*, 51(11):1217–1253.

Clark D.B., S. Elgar, and B. Raubenheimer, 2012. Vorticity generation by short-crested wave breaking. *Geophysical Research Letters*, 39(24).

Dalrymple R.A., J.H. MacMahan, J.H.M. Reniers, and Nelko V, 2011. Rip currents. *Annual Review of Fluid Mechanics*, 43:551–581.

Feddersen F. and R.T. Guza, 2003. Observations of nearshore circulation: Alongshore uniformity. *Journal of Geophysical Research: Oceans*, 108(C1):3006.

Kennedy A., Q. Chen, J. Kirby, and R. Dalrymple, 2000. Modelling of wave transformation, breaking, and runup. i: 1d. *J. Waterw. Port Coastal Ocean Eng.*, 126:39–47.

Long J.W. and H.T. Ozkan-Haller, 2005. Offshore controls on nearshore rip currents. *Journal of Geophysical Research: Oceans*, 110(C12).

Longuet-Higgins M.S. and R.W. Stewart, 1964. Radiation stresses in water waves; a physical discussion, with applications. *In Deep Sea Research and Oceanographic Abstracts*, volume 11, pages 529–562.
MacMahan J.H., E.B Thornton, and J.H.M. Reniers, 2006. Rip current review. *Coastal Engineering*, 53:191–208.
Madsen P.A., O.R. Sørensen, and H.A. Schaffer, 1997I. Surf zone dynamics simulated by a Boussinesq type model. part i. model description and cross-shore motion of regular waves. *Coastal Engineering*, 32(4): 255–287.
Madsen P.A., OR Sørensen, and HA Schaffer, 1997II. Surf zone dynamics simulated by a Boussinesq type model. part ii: Surf beat and swash oscillations for wave groups and irregular waves. *Coastal Engineering*, 32 (4):289–319.
Marchesiello P. , R. Benshila, R. Almar, Y. Uchiyama, J.C. McWilliams, and A. Shchepetkin, 2015. On tridimensional rip current modeling. *Ocean Modelling*, 96:36–48.
Michallet H. , R. Cienfuegos, E. Barthélemy, and F. Grasso, 2011. Kinematics of waves propagating and breaking on a barred beach. *Eur. J. Mech. B/Fluids*, 30:624–634.
Michallet H. , B. Castelle, E. Barthélemy, C. Berni, and P. Bonneton, 2013. Physical modeling of three-dimensional intermediate beach morphodynamics. *Journal of Geophysical Research*, 118(2):1045–1059.
Peregrine D.H., 1998 . Surf zone currents. *Theoretical and computational fluid dynamics*, 10(1-4):295–309.
Peregrine D.H., 1999. Large-scale vorticity generation by breakers in shallow and deep water. *European Journal of Mechanics-B/Fluids*, 18(3):403–408.
Raubenheimer B. , R.T. Guza, and S. Elgar, 1996. Wave transformation across the inner surf zone. J*ournal of Geophysical Research: Oceans*, 101(C11):25589–25597.
Suarez L. , R. Cienfuegos, E. Barthélemy, and H. Michallet, 2013. Vorticity evolution and related low-frequency motions on a rip-current with a non-uniform alongshore wave forcing, 2013. In *7th International Conference on Coastal Dynamics*, pages 1571–1580.
Svendsen, B., 1987. Analysis of surf zone turbulence. *Journal of Geophysical Research: Oceans*, 92(C5):5115–5124.
Thornton E.B. and R. Guza, 1983. Transformation of wave height distribution. *Journal of Geophysical Research: Oceans*, 88(C10): 5925–5938.
Weir B., Y. Uchiyama, E. M. Lane, J. M. Restrepo, and J. C. McWilliams, 2011. A vortex force analysis of the interaction of rip currents and surface gravity waves. *Journal of Geophysical Research: Oceans*, 116(C5).